Scientific Research Publishing

Open Journal of Orthopedics, 2025, 15(11), 430-449
https://www.scirp.org/journal/ojo
ISSN Online: 2164-3016
ISSN Print: 2164-3008

Effects of Combined BMP9 and bFGF Treatment on Runx2 and Col1 mRNA Expression in MC3T3-E1 Cells

Yaqiu Chen[1,2#], Yuzhao Chen[2#], Chang Liu[1], Peng Tang[3], Feng Qiu[1], Yewei Xin[1], Rilang Feng[1], Han Jiang[1], Xiaojing Sun[4], Qian Jiang[1*]

[1]The Department of Orthodontics, Affiliated Stomatology Hospital of Guilin Medical University, 109 Huancheng North 2nd Road, Qixing District, Guilin, China
[2]The College of Stomatology, Guilin Medical University, 109 Huancheng North 2nd Road, Qixing District, Guilin, China
[3]Guilin Woodpecker Medical Instrument Co. Ltd., Information lndustrial Park, National High-TechZone, Guilin, China
[4]The Department of Orthodontics, Stomatology Hospital of Guilin, No. 5 Sanduo Road, Xiufeng District, Guilin, China
Email: *200047@glmc.edu.cn

How to cite this paper: Chen, Y.Q., Chen, Y.Z., Liu, C., Tang, P., Qiu, F., Xin, Y.W., Feng, R.L., Jiang, H., Sun, X.J. and Jiang, Q. (2025) Effects of Combined BMP9 and bFGF Treatment on Runx2 and Col1 mRNA Expression in MC3T3-E1 Cells. *Open Journal of Orthopedics*, **15**, 430-449.
https://doi.org/10.4236/ojo.2025.1511044

Received: October 30, 2025
Accepted: November 25, 2025
Published: November 28, 2025

Copyright © 2025 by author(s) and Scientific Research Publishing Inc.
This work is licensed under the Creative Commons Attribution International License (CC BY 4.0).
http://creativecommons.org/licenses/by/4.0/

Open Access

Abstract

Objective: To investigate the synergistic effects of bone morphogenetic protein 9 (BMP9) and basic fibroblast growth factor (bFGF) at different concentration combinations on the mRNA expression of osteogenic markers Runx2 and Col1 in the mouse osteoblast precursor cell line MC3T3-E1. **Methods:** MC3T3-E1 cells were treated with BMP9 (10 ng/mL or 200 ng/mL) and bFGF (10 ng/mL or 100 ng/mL), either individually or in combination. Real-time quantitative PCR (qRT-PCR) was employed to measure the relative expression levels of Runx2 and Col1 mRNA at day 4 (D4) and day 7 (D7) post-treatment. **Results:** At D4, individual BMP9 treatment promoted Runx2 expression, with BMP9min (10 ng/mL) showing the strongest effect. However, combined BMP9 and bFGF treatment significantly suppressed Runx2 expression compared to BMP9 alone, indicating antagonistic interactions at this early timepoint. For Col1 expression at D4, combined treatments showed modest increases compared to negative control but remained lower than BMP9 monotherapy. At D7, while both BMP9 and bFGF monotherapy groups demonstrated significantly elevated expression of Runx2 and Col1 compared to negative control, combined treatments continued to show suppressive effects compared to BMP9 monotherapy. The presence of bFGF consistently attenuated BMP9-induced osteogenic marker expression at both timepoints. Conclusion: BMP9 and bFGF exhibit persistent antagonistic interactions in regulating osteogenic differen-

*Corresponding author.
#These authors contributed equally to this work.

tiation markers Runx2 and Col1. At both D4 and D7 timepoints, the addition of bFGF to BMP9 treatment consistently suppressed the osteogenic-promoting effects of BMP9 monotherapy, despite both growth factors showing elevated expression compared to negative control at D7. These findings challenge the presumed synergistic relationship between BMP and FGF family members and suggest that bFGF may interfere with BMP9-mediated osteogenic signaling pathways. For bone tissue engineering applications, these results indicate that careful consideration must be given to growth factor combinations, as co-delivery of BMP9 and bFGF may not enhance, and could potentially impair, osteogenic outcomes compared to BMP9 alone.

Keywords

BMP9, bFGF, MC3T3-E1 Cells, Runx2, Col1, Osteogenic Differentiation, qRT-PCR, Synergistic Effects

1. Introduction

Bone tissue regeneration and repair represent crucial research areas in orthopedics and oral medicine [1]. Osteogenic differentiation is a complex biological process involving precise regulation by multiple cellular signaling pathways and growth factors [2]. The bone morphogenetic protein (BMP) family and fibroblast growth factor (FGF) family play pivotal roles in the osteogenic process [3]. Bone morphogenetic protein 9 (BMP9) is one of the most osteogenically active members of the BMP family, capable of effectively inducing mesenchymal stem cells to differentiate into osteoblasts [4]. BMP9 activates the Smad-dependent signaling pathway, upregulating the expression of osteogenesis-related transcription factors and markers, thereby promoting bone matrix formation and mineralization [5]. Basic fibroblast growth factor (bFGF, also known as FGF2) is an important member of the FGF family and plays multifaceted roles in bone development and fracture healing. bFGF promotes the proliferation of osteoblast precursor cells and influences osteogenic differentiation under specific conditions. Runx2 (Runt-related transcription factor 2) serves as the master regulator of osteogenic differentiation and is essential for osteoblast differentiation and bone formation [6]. Type I collagen (Collagen type I, Col 1) is the major protein component of bone matrix, and its expression level reflects the maturity of osteoblasts and their capacity for bone matrix synthesis [7]. These two markers are commonly used as important indicators for assessing the degree of osteogenic differentiation.

Although the individual osteogenic effects of BMP9 and bFGF have been extensively studied, the synergistic effects of their combined application on osteogenic differentiation require further investigation. Based on the reported synergistic interactions between BMP and FGF family members in bone formation, we hypothesize that the combination of BMP9 and bFGF will produce a synergistic effect, significantly enhancing the expression of osteogenic markers Runx2 and Col1.

This study aims to evaluate the effects of different concentrations of BMP9 and bFGF combinations on the mRNA expression of Runx2 and Col1 in MC3T3-E1 cells using real-time quantitative PCR technology, thereby providing experimental evidence for optimizing bone tissue engineering strategies.

2. Materials and Methods

2.1. Cell Culture

MC3T3-E1 mouse osteoblast precursor cells were purchased from the Cell Bank of the Chinese Academy of Sciences. Cells were cultured in α-MEM medium containing 10% fetal bovine serum, 100 U/mL penicillin, and 100 μg/mL streptomycin, and maintained in a cell culture incubator at 37˚C with 5% CO_2. When cell confluence reached 80% - 90%, cells were passaged or subjected to experimental treatment.

2.2. Experimental Groups and Treatment

The following treatment groups were established:

1) Control group: α-MEM medium (Complete Medium, CM) containing 2%FBS

2) 10 ng/ml bFGF: CM + 10 ng/ml bFGF

3) 100 ng/ml bFGF: CM + 100 ng/ml bFGF

4) 10 ng/ml BMP9: CM + 10 ng/ml BMP9

5) 200 ng/ml BMP9: CM + 200 ng/ml BMP9

6) 10 ng/ml bFGF + 10 ng/ml BMP9: CM + 10 ng/ml bFGF + 10 ng/ml BMP9

7) 10 ng/ml bFGF + 200 ng/ml BMP9: CM + 10 ng/ml bFGF + 200 ng/ml BMP9

8) 100 ng/ml bFGF + 10 ng/ml BMP9: CM + 100 ng/ml bFGF + 10 ng/ml BMP9

9) 100 ng/ml bFGF + 200 ng/ml BMP9: CM + 100 ng/ml bFGF + 200 ng/ml BMP9

Cells were cultured under different treatment conditions and harvested on day 4 (D4) and day 7 (D7) for subsequent RNA extraction and gene expression analysis.

2.3. RNA Extraction and cDNA Synthesis

Total RNA was extracted from cells using TRIzol reagent (Solarbio, China) according to the manufacturer's instructions. RNA concentration and purity were measured using a NanoDrop 2000 spectrophotometer (Thermo Scientific, USA). RNA samples with A260/A280 ratios between 1.8 - 2.0 were used for subsequent experiments. Reverse transcription was performed using the ToloScript All-in-one RT EasyMix for qPCR (Tolobio, China) to synthesize first-strand cDNA. The reverse transcription system was 20 μL, with reaction conditions of 37˚C for 15 minutes, 85˚C for 5 seconds, and storage at 4˚C.

2.4. Real-Time Quantitative PCR

qRT-PCR was performed using the SYBR Green method. The reaction system was

20 μL, containing 10 μL SYBR Green premix, 1 μL cDNA template, 0.4 μL forward and reverse primers (10 μM each), and 8.2 μL ddH_2O. The reaction program consisted of: 95˚C pre-denaturation for 30 seconds, followed by 40 cycles of 95˚C denaturation for 5 seconds and 60˚C annealing-extension for 34 seconds. Three technical replicates were performed for each sample. GAPDH was used as the internal reference gene, and the $2^{-\Delta\Delta ct}$ method was employed to calculate the relative expression levels of target genes in Table 1.

Table 1. Primers for RT-PCR.

Gene	Reverse Primer (5'-3')
Col 1	F: ATCCTGCCGATGTCGCTATCC
	R: TTCTTGAGGTTGCCAGTCTGTTG
Runx2	F: GTCCGCCACCACTCACTACC
	R: ACGCTGACGAAGTACCATAGTAGAG
GAPDH	F: AAGTTCAACGGCACAGTCAAGG
	R: GACATACTCAGCACCAGCATCAC

2.5. Statistical Analysis

Experimental data are expressed as mean ± standard deviation (Mean ± SD). Statistical analysis was performed using GraphPad Prism 9.0 software. Multiple group comparisons were conducted using one-way ANOVA, and pairwise comparisons between groups were performed using Tukey's multiple comparison test. $P < 0.05$ was considered statistically significant, where *P < 0.05, **P < 0.01, ***P < 0.001, ****P < 0.0001, and ns indicates no statistical difference.

3. Results

3.1. Effects of BMP9 and bFGF on Runx2 mRNA Expression

3.1.1. Runx2 Expression at Day 4: Comparison with Negative Control

At the D4 timepoint, distinct expression patterns were observed across treatment groups (Figure 1). The BMP9min (10 ng/mL) group exhibited the highest Runx2 expression, exceeding the negative control (NC) group. The BMP9max (200 ng/mL) group also showed elevated expression compared to NC, though to a lesser extent than BMP9min. Notably, all combined treatment groups (bFGFmin + BMP9min, bFGFmin + BMP9max, bFGFmax + BMP9min, and bFGFmax + BMP9max) demonstrated significantly lower Runx2 expression compared to NC, indicating that dual-factor intervention suppressed Runx2 expression at this early timepoint.

3.1.2. Runx2 Expression at D4: Intra-group Comparisons

Pairwise comparisons within the combined treatment groups (Figure 2(a)) revealed no statistically significant differences, suggesting that after 4 days of intervention, variations in BMP9 and bFGF concentrations did not substantially alter

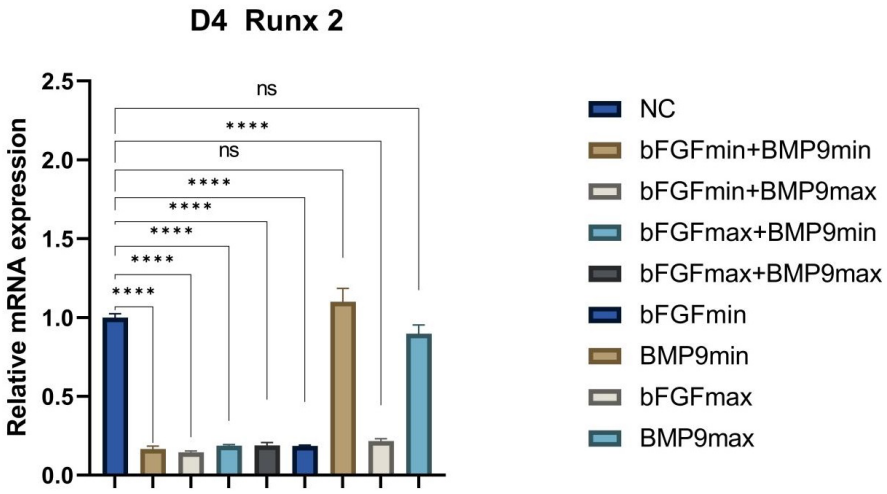

Figure 1. Runx2 expression at Day 4: Comparison with negative control

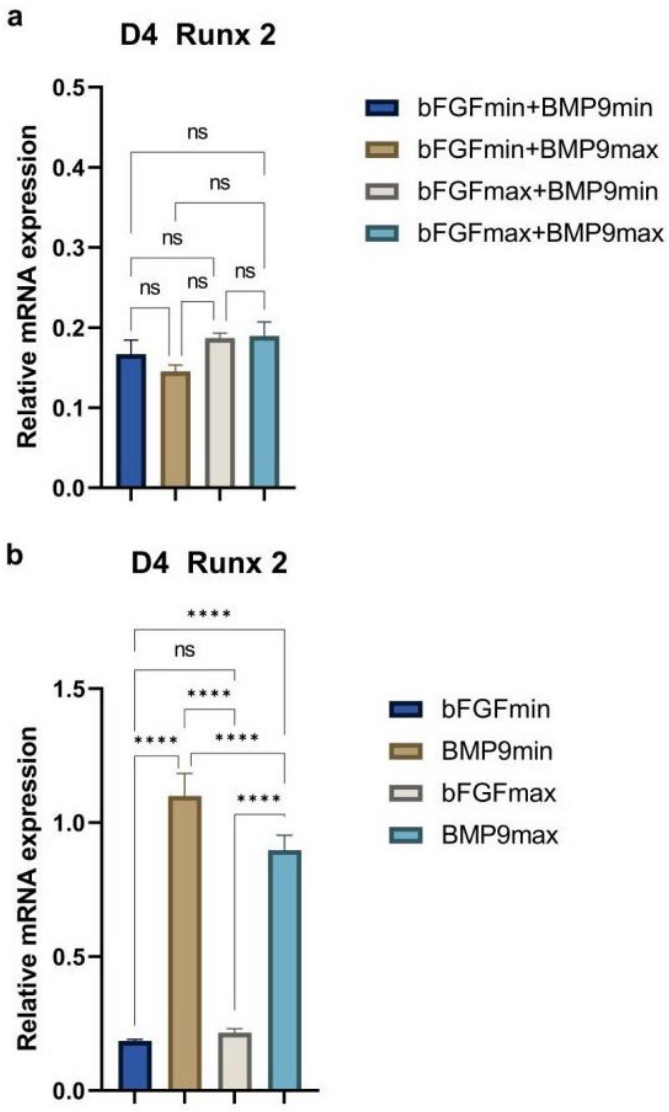

Figure 2. Runx2 expression at D4: Intra-group comparisons.

Runx2 expression levels in combination therapies. However, within the monotherapy groups (Figure 2(b)), BMP9 treatment significantly promoted Runx2 expression compared to bFGF treatment (****P < 0.0001). Importantly, BMP9min demonstrated greater promotional effects than BMP9max, indicating an inverse dose-response relationship at this timepoint.

3.1.3. Runx2 Expression at D4: Monotherapy versus Combination Therapy

Comparison between bFGF monotherapy and bFGF-containing combination groups (Figure 3(a)) showed no significant differences, suggesting that bFGF alone does not enhance Runx2 expression at D4. In contrast, comparing BMP9 monotherapy with BMP9-containing combination groups (Figure 3(b)) revealed significant differences (****P < 0.0001), with monotherapy groups showing substantially higher expression. This indicates that the addition of bFGF to BMP9 treatment suppresses BMP9's promotional effect on Runx2 at the early stage.

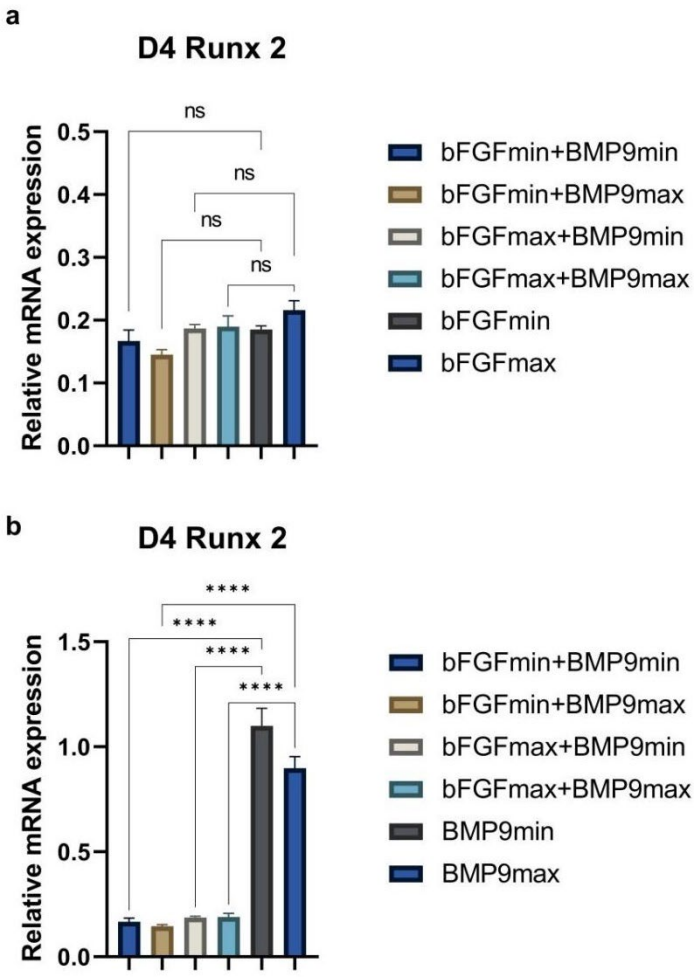

Figure 3. Runx2 expression at D4: Monotherapy versus combination therapy.

3.1.4. Runx2 Expression at Day 7: Comparison with Negative Control

At D7, enhanced osteogenic activity was evident in specific treatment groups (Fig-

ure 4). BMP9 monotherapy groups (both BMP9min and BMP9max) demonstrated significantly elevated Runx2 expression compared to NC (****P < 0.0001), confirming BMP9's robust osteogenic potency. bFGF monotherapy groups also showed increased expression relative to NC. However, importantly, all combination treatment groups exhibited Runx2 expression levels below NC, indicating that bFGF's suppressive effect on BMP9-induced Runx2 expression persisted at this later timepoint. Despite the extended culture duration, the antagonistic interaction between BMP9 and bFGF remained pronounced, with combination treatments failing to achieve even baseline osteogenic marker expression.

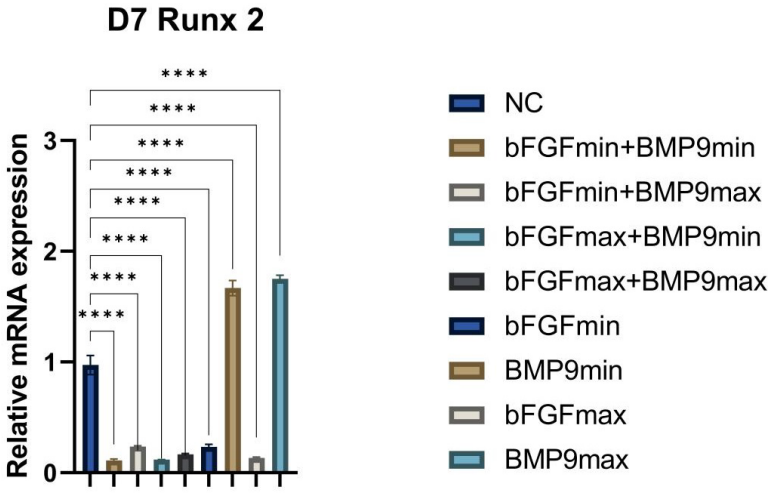

Figure 4. Runx2 expression at Day 7: Comparison with negative control.

3.1.5. Runx2 Expression at D7: Intra-group Comparisons

Within the combined treatment groups at D7 (**Figure 5(a)**), no statistically significant differences were observed among the four combination groups, suggesting that different concentration combinations produced comparable effects. Among monotherapy groups (**Figure 5(b)**), BMP9 treatments (both min and max) significantly outperformed bFGF treatments (****P < 0.0001), confirming BMP9's superior osteogenic potency. Notably, BMP9 monotherapy groups achieved higher Runx2 expression levels than any combination group.

3.1.6. Runx2 Expression at D7: Monotherapy versus Combination Therapy

At D7, comparison between bFGF monotherapy and bFGF-containing combination groups (**Figure 6(a)**) showed that combinations produced higher expression than bFGF alone, indicating that BMP9's osteogenic effects were partially retained even in the presence of bFGF. However, critically, comparing BMP9 monotherapy with BMP9-containing combination groups (**Figure 6(b)**) revealed that BMP9 alone significantly outperformed all combination treatments (****P < 0.0001). This demonstrates that the addition of bFGF consistently attenuated BMP9's promotional effects on Runx2 expression, confirming persistent antagonistic interactions at D7.

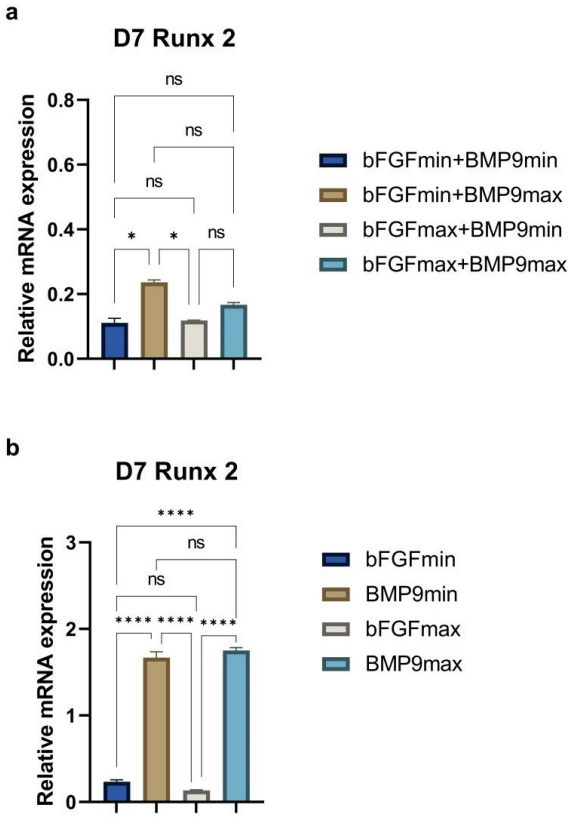

Figure 5. Runx2 expression at D7: Intra-group comparisons.

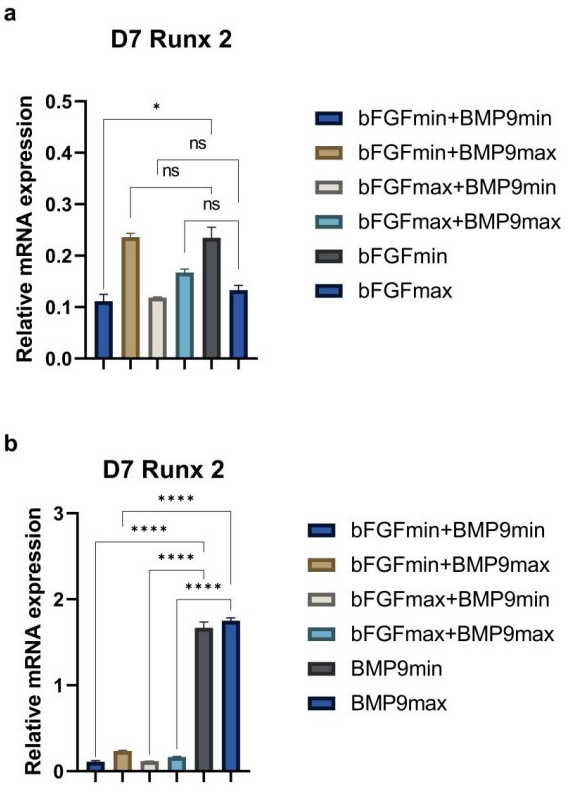

Figure 6. Runx2 expression at D7: Monotherapy versus combination therapy.

3.1.7. Temporal Comparison: D4 versus D7

Temporal analysis (Figure 7) revealed distinct expression trajectories for different treatment groups. BMP9 monotherapy groups showed substantial increases in Runx2 expression from D4 to D7 (****P < 0.0001), indicating progressive osteogenic differentiation. bFGF monotherapy also showed modest increases over time. Combination therapy groups exhibited increases from D4 to D7, but their final expression levels at D7 remained significantly lower than BMP9 monotherapy at both timepoints. This temporal pattern confirms that bFGF's interference with BMP9-mediated Runx2 upregulation is not a transient early-stage phenomenon but rather a sustained effect throughout the differentiation process.

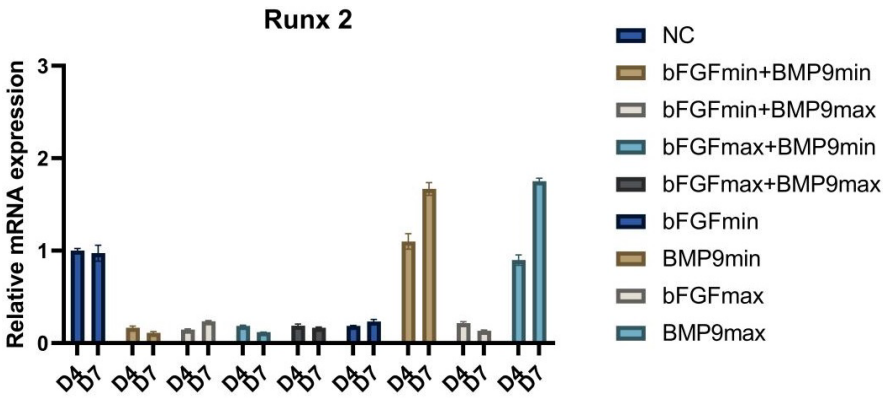

Figure 7. Temporal comparison: D4 versus D7.

3.2. Effects of BMP9 and bFGF on Col1 mRNA Expression

3.2.1. Col1 Expression at Day 4: Comparison with Negative Control

At D4 (Figure 8), Col1 expression patterns showed similar antagonistic trends as observed with Runx2. BMP9 monotherapy groups demonstrated the highest Col1 expression, significantly exceeding NC levels, confirming BMP9's early promotional effect on matrix protein production. In contrast, all combination treatment

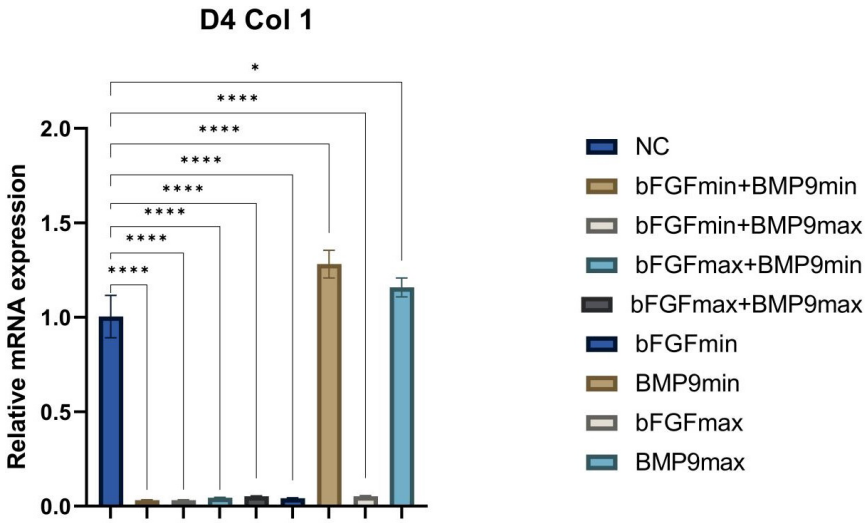

Figure 8. Col1 expression at Day 4: Comparison with negative control.

groups (bFGFmin + BMP9min, bFGFmin + BMP9max, bFGFmax + BMP9min, and bFGFmax + BMP9max) exhibited Col1 expression levels substantially below NC, indicating that bFGF presence suppressed both BMP9-induced and baseline Col1 expression at this early timepoint. bFGF monotherapy alone also showed minimal Col1 expression, remaining below NC levels. These findings demonstrate that the antagonistic interaction between BMP9 and bFGF affects not only the early commitment marker Runx2 but also extends to downstream matrix production markers as early as D4.

3.2.2. Col1 Expression at D4: Intra-Group Comparisons

Within combined treatment groups at D4 (**Figure 9(a)**), pairwise comparisons showed relatively uniform Col1 expression levels with some statistical differences between specific combinations. Among monotherapy groups (**Figure 9(b)**), BMP9 treatments significantly promoted Col1 expression compared to bFGF treatments (****$P < 0.0001$), with both BMP9min and BMP9max showing comparable effects.

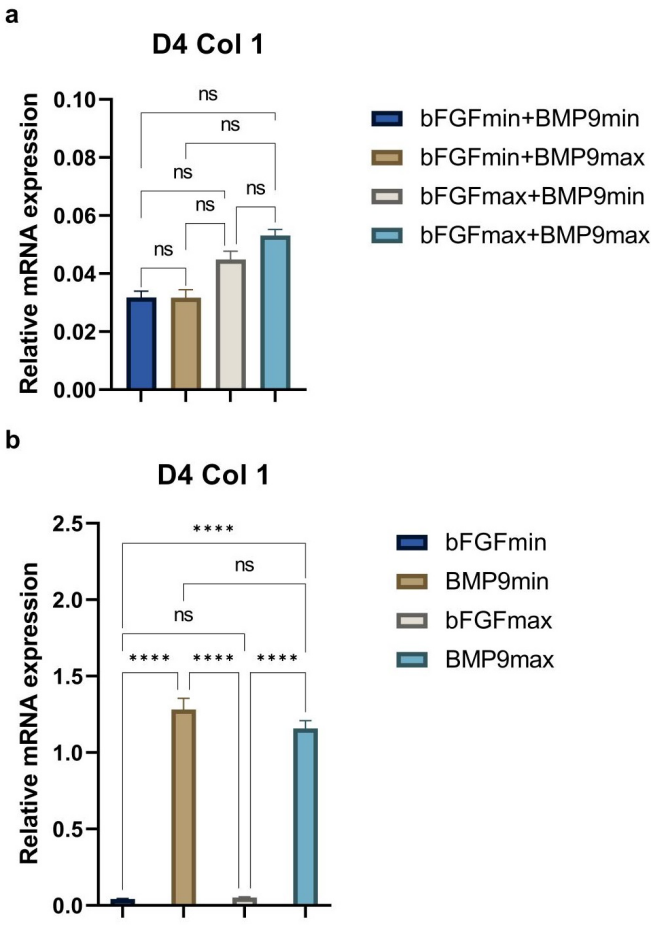

Figure 9. Col1 expression at D4: Intra-group comparisons.

3.2.3. Col1 Expression at D4: Monotherapy versus Combination Therapy

Comparing bFGF monotherapy with bFGF-containing combinations (**Figure 10(a)**) revealed no significant promotional effect of bFGF on Col1 expression at

D4. However, BMP9 monotherapy versus BMP9-containing combinations (Figure 10(b)) showed that BMP9 alone produced higher Col1 expression than combination treatments (***P < 0.001 to ****P < 0.0001), suggesting that bFGF attenuates BMP9's effect on Col1 at this early timepoint.

3.2.4. Col1 Expression at Day 7: Comparison with Negative Control

At D7 (Figure 11), BMP9 monotherapy groups demonstrated the highest Col1

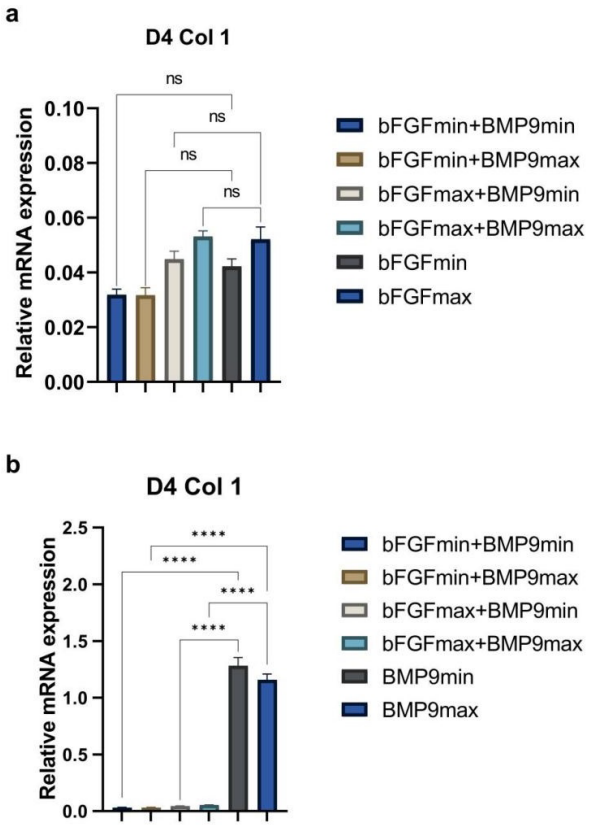

Figure 10. Col1 expression at D4: Monotherapy versus combination therapy.

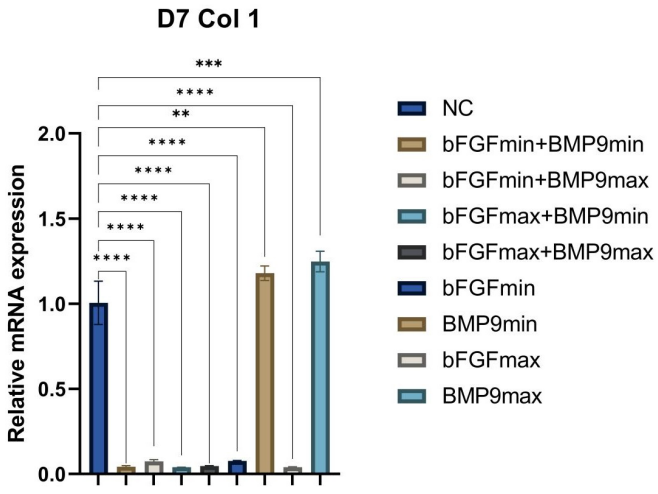

Figure 11. Col1 expression at Day 7: Comparison with negative control.

expression levels (****P < 0.0001), indicating robust matrix production capacity. However, combination treatment groups exhibited Col1 expression levels below NC, demonstrating that bFGF's antagonistic effect on BMP9-induced Col1 expression remained pronounced at D7. This pattern parallels the Runx2 results, confirming that the suppressive interaction between BMP9 and bFGF affects both early transcriptional regulators and late-stage matrix production markers.

3.2.5. Col1 Expression at D7: Comprehensive Comparisons

Within combination groups at D7 (Figure 12), different concentration combinations showed relatively similar Col1 expression levels with some variations, but none achieved the expression levels of BMP9 monotherapy. Among monotherapies, BMP9 groups significantly exceeded bFGF groups (****P < 0.0001), confirming BMP9's dominant role in promoting Col1 expression.

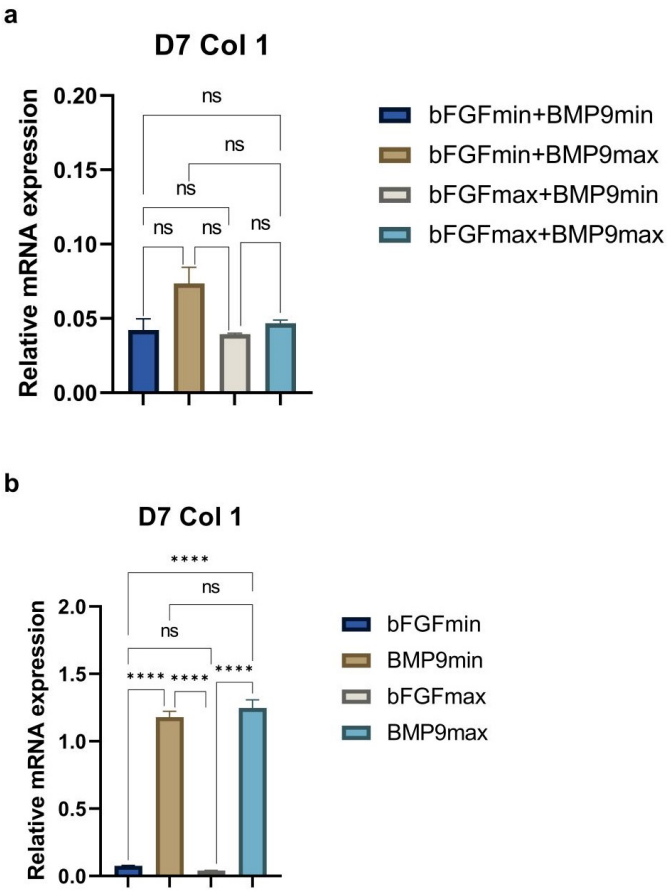

Figure 12. Col1 expression at D7: Comprehensive comparisons.

3.2.6. Col1 Expression at D7: Comprehensive Comparisons

Comparing monotherapy versus combination therapy at D7 (Figure 13), combination groups containing bFGF showed lower Col1 expression than BMP9 monotherapy groups (****P < 0.0001), although they exceeded bFGF monotherapy alone. This pattern reinforces that while bFGF does not completely abolish BMP9's osteogenic effects, it significantly diminishes them.

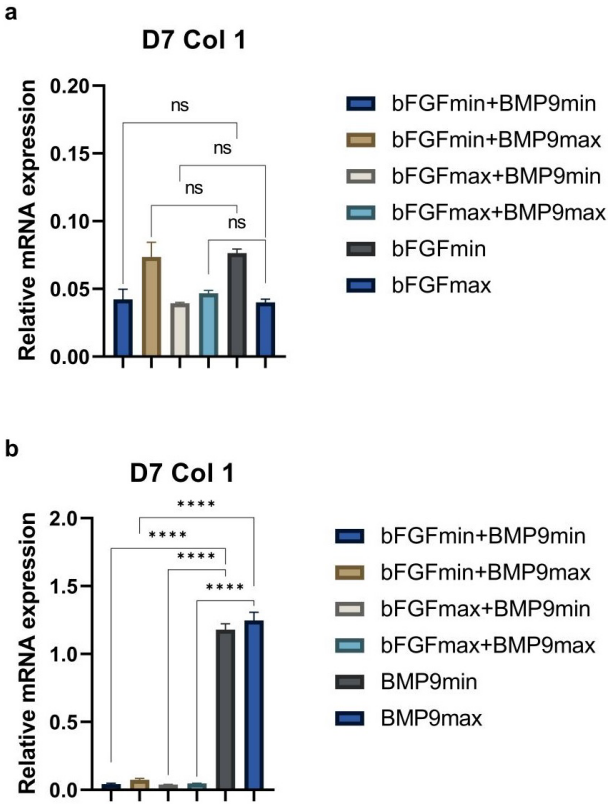

Figure 13. Col1 expression at D7: Comprehensive comparisons.

3.2.7. Temporal Comparison: D4 versus D7

Temporal analysis of Col1 expression (Figure 14) revealed that BMP9 monotherapy groups exhibited substantial increases from D4 to D7 (****P < 0.0001), reflecting progressive osteoblast maturation and enhanced matrix synthesis capability. Combination therapy groups also showed increases over time, but their D7 expression levels remained below those of BMP9 monotherapy. This temporal pattern parallels the Runx2 results, indicating that bFGF's attenuating effect on BMP9-induced osteogenic differentiation persists throughout the culture period and affects both early commitment markers (Runx2) and late differentiation/functional markers (Col1).

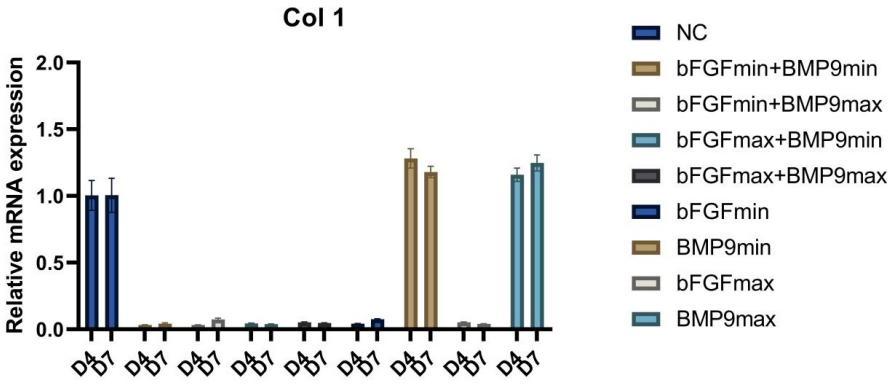

Figure 14. Temporal comparison: D4 versus D7.

4. Discussion

4.1. Antagonistic Interactions Between BMP9 and bFGF in Osteogenic Differentiation

This study reveals consistent antagonistic interactions between BMP9 and bFGF throughout the osteogenic differentiation process. Contrary to the commonly hypothesized synergistic relationship between BMP and FGF family members in bone formation, our data demonstrate that bFGF persistently attenuates BMP9's promotional effects on osteogenic marker expression at both early (D4) and late (D7) timepoints. At D4, BMP9 monotherapy, particularly at the lower concentration (10 ng/mL), significantly upregulated Runx2 expression above negative control levels. However, all BMP9 + bFGF combination groups showed Runx2 expression below negative control, indicating that bFGF not only neutralized BMP9's effects but actively suppressed baseline osteogenic commitment. This profound early-stage antagonism suggests fundamental signaling pathway interference. At D7, BMP9 monotherapy and bFGF monotherapy demonstrated elevated expression of both Runx2 and Col1 compared to negative control, reflecting their individual osteogenic contributions. However, combination treatment groups remained below negative control levels for both markers, demonstrating that the antagonistic relationship between BMP9 and bFGF persisted throughout the differentiation period. BMP9 monotherapy consistently achieved the highest expression levels, and the addition of bFGF at any concentration not only eliminated BMP9's promotional effects but actively suppressed expression below baseline levels. This sustained antagonism indicates that bFGF's interference with BMP9 signaling is not a transient phenomenon limited to early commitment stages but rather affects the entire differentiation trajectory, including late-stage matrix production [8] [9].

The molecular basis for this antagonism likely involves multiple mechanisms. BMP9 signals primarily through BMP type I receptors ALK1 and ALK2, activating Smad1/5/8 phosphorylation and subsequent nuclear translocation to drive transcription of osteogenic genes including Runx2 [10]. bFGF, conversely, signals through FGF receptors (FGFRs) to activate multiple pathways including MAPK/ERK, PI3K/AKT, and PLC γ . Critically, sustained ERK activation by FGF signaling has been shown to inhibit BMP-induced osteogenesis through several mechanisms: 1) Linker region phosphorylation: ERK can phosphorylate the linker regions of Smad1/5/8, marking them for ubiquitination and proteasomal degradation, thereby reducing the pool of Smads available for BMP9 signaling. 2) Transcriptional interference: Activated ERK can phosphorylate transcription factors that compete with Smad complexes for binding to osteogenic gene promoters, effectively blocking BMP-mediated transcriptional activation. 3) Receptor regulation: Chronic FGF signaling can downregulate BMP receptor expression or alter their trafficking and localization, reducing cellular responsiveness to BMP9. 4) Induction of inhibitory factors: bFGF can induce expression of BMP antagonists such as Noggin or inhibitory Smads (Smad6/7), which directly block BMP signaling.

4.2 Parallel Regulation of Runx2 and Col1 Expression

Our results demonstrate that Runx2 and Col1 respond similarly to BMP9 and bFGF combinations, with both markers showing the same pattern of BMP9 promotion and bFGF-mediated attenuation. This parallel regulation differs from scenarios where early and late osteogenic markers show divergent responses to growth factor combinations.

Runx2, as the master transcription factor for osteogenesis, is directly regulated by BMP-Smad signaling [11]. Smad complexes bind to osteoblast-specific cis-regulatory elements (OSE) in the Runx2 promoter, driving its transcription [12]. The suppression of Runx2 by bFGF + BMP9 combinations indicates that FGF signaling effectively blocks this BMP-Smad transcriptional activation.

Col1, while a downstream target in the osteogenic cascade, shows remarkably similar sensitivity to the BMP9-bFGF interaction [13]. At both D4 and D7, Col1 expression patterns mirror those of Runx2: BMP9 monotherapy produces the highest expression, while bFGF addition reduces these levels below even negative control at D7. This parallel response suggests that bFGF's antagonistic effect operates at multiple levels—both on the master regulator (Runx2) and on downstream effectors (Col1).

The consistent suppression of Col1 despite its position downstream in the differentiation cascade is particularly significant [14]. Col1 expression is regulated not only by Runx2 but also by other transcription factors including Sp1, Sp3, and AP-1 family members, some of which can be modulated by MAPK signaling [15]. The fact that bFGF attenuates Col1 expression suggests either that: (1) the reduction in Runx2 is sufficient to limit Col1 transcription, indicating Runx2's dominant role, or (2) bFGF-activated pathways directly interfere with Col1 transcriptional machinery beyond Runx2-mediated regulation. It should be noted that a limitation is that all conclusions are based entirely on mRNA expression levels. The mRNA levels may not perfectly correlate with protein expression and functional activity. Nevertheless, this observation lays the groundwork for subsequent investigations focused on protein-level analysis.

4.3. Concentration-Dependent Effects and Dose-Response Relationships

The concentration-dependent analysis revealed important nuances in growth factor activity and interactions [16]. At D4, BMP9min (10 ng/mL) produced greater Runx2 upregulation than BMP9max (200 ng/mL), indicating a non-linear or inverse dose-response relationship. This phenomenon is not uncommon in BMP signaling and may result from several mechanisms: 1) Receptor saturation and internalization: Higher BMP9 concentrations may lead to excessive receptor occupancy, triggering rapid receptor internalization and degradation, paradoxically reducing sustained signaling. 2) Negative feedback activation: High BMP concentrations can strongly induce inhibitory Smad6 and Smad7 expression, which function as negative feedback regulators by preventing R-Smad phosphorylation and

promoting BMP receptor degradation. 3) Non-canonical pathway activation: At high concentrations, BMP9 may preferentially activate non-Smad pathways (such as p38 MAPK or TAK1) that can have context-dependent effects on osteogenic gene expression. At D7, the dose-response relationship became more conventional for BMP9 monotherapy, with both concentrations showing strong effects. However, the antagonistic effect of bFGF remained concentration-independent within the tested ranges—both low and high concentrations of bFGF similarly attenuated BMP9's effects, and different combination ratios produced comparable results [6]. This suggests that bFGF's interference mechanism is saturated even at the lower concentration (10 ng/mL), and that increasing bFGF or BMP9 concentrations does not overcome the antagonism.

The lack of a "rescue effect" at higher BMP9 concentrations in combination treatments is particularly notable. One might hypothesize that increasing BMP9 levels could outcompete bFGF's inhibitory effects through mass action. The absence of such rescue suggests that bFGF's antagonism operates through mechanisms that cannot be simply overcome by increasing BMP9 receptor occupancy—such as downstream signaling interference, transcriptional competition, or sustained ERK-mediated Smad degradation [17].

4.4. Implications for Bone Tissue Engineering

These findings have important practical implications for bone tissue engineering and regenerative medicine strategies. The persistent antagonistic interactions between BMP9 and bFGF across both early and late differentiation stages suggest that simultaneous co-delivery of these growth factors may be counterproductive for osteogenic applications [18]. The synergistic effect observed when BMP-2 and bFGF are used in combination [19]. On the contrary, our data clearly demonstrate that BMP9 monotherapy consistently outperforms BMP9 + bFGF combinations at both D4 and D7 timepoints for both Runx2 and Col1 expression. This indicates that the simple addition of bFGF to BMP9-based bone regeneration strategies will not enhance, and may actually impair, osteogenic outcomes [20]. This challenges the prevalent assumption in tissue engineering that combining multiple growth factors will produce additive or synergistic benefits. For clinical applications, these results suggest several strategic considerations: 1) BMP9 monotherapy may be preferable: Given BMP9's superior performance alone, bone regeneration scaffolds may achieve better outcomes with BMP9 as the sole osteogenic factor rather than BMP9 + bFGF combinations. 2) Temporal separation strategies: If both factors are desired—bFGF for its angiogenic and cell proliferation effects, and BMP9 for osteogenesis—sequential delivery systems may be necessary. Biomaterial scaffolds could be designed to release bFGF initially to expand progenitor cell populations and promote vascularization, followed by complete clearance of bFGF before BMP9 release to drive differentiation without interference. Critically, a temporal gap between factor deliveries would be essential to avoid overlap. 3) Spatial compartmentalization: Alternative approaches might involve spatial separation where bFGF is

delivered to peripheral scaffold regions to promote vascularization and cell recruitment, while BMP9 is concentrated in core regions designated for bone formation, minimizing direct interaction between the two factors. 4) Mechanistic interventions: Future strategies might attempt to preserve bFGF's beneficial effects (cell proliferation, angiogenesis) while blocking its antagonistic effects on BMP9 signaling. This could involve co-delivery of ERK pathway inhibitors, use of bFGF variants with altered signaling properties, or development of BMP9 variants resistant to FGF-mediated antagonism.

The concentration-dependent effects observed, particularly the inverse dose-response of BMP9 at D4, highlight the need for precise growth factor dosing in clinical applications [21]. The finding that neither increasing BMP9 concentration nor decreasing bFGF concentration could rescue the antagonistic effect in combination treatments suggests that even low-level bFGF exposure can significantly compromise BMP9 efficacy. These results emphasize that assessing bone regeneration strategies requires comprehensive evaluation across multiple timepoints and markers [22]. The consistent antagonism observed for both early commitment markers (Runx2) and late functional markers (Col1) indicates that bFGF's interference affects the entire osteogenic program, from initial lineage commitment through matrix production [23]. This has important implications for predicting in vivo outcomes, as even modestly reduced marker expression in vitro may translate to substantially impaired bone formation and mineralization in clinical settings [24].

5. Conclusion

This study reveals persistent antagonistic interactions between BMP9 and bFGF in regulating osteogenic differentiation, with bFGF consistently attenuating BMP9's promotional effects on Runx2 and Col1 expression at both early and late differentiation stages. The antagonism likely involves MAPK/ERK-mediated interference with BMP-Smad signaling and could not be overcome by concentration adjustments [25]. For bone tissue engineering applications, these findings challenge the assumption that combining growth factors from different families produces synergistic benefits and suggest that simultaneous co-delivery of BMP9 and bFGF may impair rather than enhance osteogenic outcomes [26]. If both factors are required, temporal separation or spatial compartmentalization strategies would be necessary to prevent antagonistic interactions and optimize bone regeneration efficacy.

Acknowledgments

This work was supported by Project to improve basic research ability of young and middle-aged teachers in Guangxi colleges and universities (No.2024KY0499), Guilin Science Research and Technology Development Program(No.20230135-5-1),Guangxi Medical and Health Appropriate Technology Development and Application Project (No.S2022153), Guangxi Zhuang Autonomous Region Health

Commission self-funded research project (No.Z-C20231971). Guangxi Zhuang Autonomous Region College Students' Innovation and Entrepreneurship Training Program (No.S202410601194). Graduate Research Program of Guilin Medical University (No.GYYK2025025).

Contribution

YQ. C, YZ. C, YW. X and P.T contributed to the drafting of the manuscript; YQ. C, YZ. C and Q.J contributed to the conception and design of study; C.L, RL.F, H.J and XJ.S contributed to the experimental research and data analyse; Q.F contributed to the supervision of study. All authors approved the version submitted for publication. All authors read and approved the final manuscript.

Conflicts of Interest

The authors declare no conflicts of interest regarding the publication of this paper.

References

[1] Mandal, B.B., Grinberg, A., Seok Gil, E., Panilaitis, B. and Kaplan, D.L. (2012) High-strength Silk Protein Scaffolds for Bone Repair. *Proceedings of the National Academy of Sciences*, **109**, 7699-7704. https://doi.org/10.1073/pnas.1119474109

[2] Sun, L., Chen, J., Li, L.J. and Li, L. (2024) Similarity-Based Metric Analysis Approach for Predicting Osteogenic Differentiation Correlation Coefficients and Discovering the Novel Osteogenic-Related Gene FOXA1 in BMSCs. *Peer Journal*, **12**, e18068. https://doi.org/10.7717/peerj.18068

[3] Mishina, Y. and Snider, T.N. (2014) Neural Crest Cell Signaling Pathways Critical to Cranial Bone Development and Pathology. *Experimental Cell Research*, **325**, 138-147. https://doi.org/10.1016/j.yexcr.2014.01.019

[4] Wu, N., Zhao, Y., Yin, Y., Zhang, Y. and Luo, J. (2010) Identification and Analysis of Type II TGF-β Receptors in BMP-9-Induced Osteogenic Differentiation of C3H10T1/2 Mesenchymal Stem Cells. *Acta Biochimica et Biophysica Sinica*, **42**, 699-708. https://doi.org/10.1093/abbs/gmq075

[5] Zhu, L., Liu, Y., Wang, A., Zhu, Z., Li, Y., Zhu, C., *et al.* (2022) Application of BMP in Bone Tissue Engineering. *Frontiers in Bioengineering and Biotechnology*, **10**, Article 810880. https://doi.org/10.3389/fbioe.2022.810880

[6] Luo, G., Xu, B., Wang, W., Wu, Y. and Li, M. (2018) Study of the Osteogenesis Effect of Icariside II and Icaritin on Canine Bone Marrow Mesenchymal Stem Cells. *Journal of Bone and Mineral Metabolism*, **36**, 668-678. https://doi.org/10.1007/s00774-017-0889-5

[7] Miao, S., Zhou, J., Liu, B., Lei, X., Wang, T., Hao, X., *et al.* (2022) A 3D Bioprinted Nano-Laponite Hydrogel Construct Promotes Osteogenesis by Activating PI3K/AKT Signaling Pathway. *Materials Today Bio*, **16**, Article 100342. https://doi.org/10.1016/j.mtbio.2022.100342

[8] Lim, S., Ihn, H.J., Kim, J.A., Bae, J., Kim, J., Bae, Y.C., *et al.* (2023) Suppressive Effects of (-)-Tubaic Acid on RANKL-Induced Osteoclast Differentiation and Bone Resorption. *Animal Cells and Systems*, **27**, 1-9. https://doi.org/10.1080/19768354.2023.2166107

[9] Gahan, J.M., Schnitzler, C.E., DuBuc, T.Q., Doonan, L.B., Kanska, J., Gornik, S.G., *et*

al. (2017) Functional Studies on the Role of Notch Signaling in Hydractinia Development. *Developmental Biology*, **428**, 224-231. https://doi.org/10.1016/j.ydbio.2017.06.006

[10] Song, T., Wang, W., Xu, J., Zhao, D., Dong, Q., Li, L., *et al.* (2013) Fibroblast Growth Factor 2 Inhibits Bone Morphogenetic Protein 9-Induced Osteogenic Differentiation of Mesenchymal Stem Cells by Repressing Smads Signaling and Subsequently Reducing Smads Dependent Up-Regulation of ALK1 and ALK2. *The International Journal of Biochemistry & Cell Biology*, **45**, 1639-1646. https://doi.org/10.1016/j.biocel.2013.05.005

[11] Wu, M., Wu, S., Chen, W. and Li, Y. (2024) The Roles and Regulatory Mechanisms of TGF-β and BMP Signaling in Bone and Cartilage Development, Homeostasis and Disease. *Cell Research*, **34**, 101-123. https://doi.org/10.1038/s41422-023-00918-9

[12] Abdullah, A.R., Hapidin, H. and Abdullah, H. (2018) The Role of Semi-Purified Fractions Isolated from *Quercus infectoria* on Bone Metabolism by Using hFOB 1.19 Human Fetal Osteoblast Cell Model. *Evidence-Based Complementary and Alternative Medicine*, **2018**, Article 5319528. https://doi.org/10.1155/2018/5319528

[13] Zhang, J., Weng, Y., Liu, X., Wang, J., Zhang, W., Kim, S.H., *et al.* (2013) Endoplasmic Reticulum (ER) Stress Inducible Factor Cysteine-Rich with EGF-Like Domains 2 (Creld2) Is an Important Mediator of BMP9-Regulated Osteogenic Differentiation of Mesenchymal Stem Cells. *PLOS ONE*, **8**, e73086. https://doi.org/10.1371/journal.pone.0073086

[14] Kuwajima, M., Kumano, G. and Nishida, H. (2014) Regulation of the Number of Cell Division Rounds by Tissue-Specific Transcription Factors and CDK Inhibitor during Ascidian Embryogenesis. *PLOS ONE*, **9**, e90188. https://doi.org/10.1371/journal.pone.0090188

[15] Basque, A., Nguyen, H.T., Touaibia, M. and Martin, L.J. (2021) Gigantol Improves Cholesterol Metabolism and Progesterone Biosynthesis in MA-10 Leydig Cells. *Current Issues in Molecular Biology*, **44**, 73-93. https://doi.org/10.3390/cimb44010006

[16] Kikuchi, N., Yoshioka, T., Taniguchi, Y., Sugaya, H., Arai, N., Kanamori, A., *et al.* (2019) Optimization of Leukocyte-Poor Platelet-Rich Plasma Preparation: A Validation Study of Leukocyte-Poor Platelet-Rich Plasma Obtained Using Different Preparer, Storage, and Activation Methods. *Journal of Experimental Orthopaedics*, **6**, Artilce 24. https://doi.org/10.1186/s40634-019-0190-8

[17] Meng, X., Vander Ark, A., Lee, P., Hostetter, G., Bhowmick, N.A., Matrisian, L.M., *et al.* (2016) Myeloid-Specific TGF-β Signaling in Bone Promotes Basic-FGF and Breast Cancer Bone Metastasis. *Oncogene*, **35**, 2370-2378. https://doi.org/10.1038/onc.2015.297

[18] Bai, Y., Li, P., Yin, G., Huang, Z., Liao, X., Chen, X., *et al.* (2013) BMP-2, VEGF and bFGF Synergistically Promote the Osteogenic Differentiation of Rat Bone Marrow-Derived Mesenchymal Stem Cells. *Biotechnology Letters*, **35**, 301-308. https://doi.org/10.1007/s10529-012-1084-3

[19] Wang, L., Huang, Y., Pan, K., Jiang, X. and Liu, C. (2010) Osteogenic Responses to Different Concentrations/Ratios of BMP-2 and bFGF in Bone Formation. *Annals of Biomedical Engineering*, **38**, 77-87. https://doi.org/10.1007/s10439-009-9841-8

[20] Shui, W., Zhang, W., Yin, L., Nan, G., Liao, Z., Zhang, H., *et al.* (2014) Characterization of Scaffold Carriers for BMP9-Transduced Osteoblastic Progenitor Cells in Bone Regeneration. *Journal of Biomedical Materials Research Part A*, **102**, 3429-3438. https://doi.org/10.1002/jbm.a.35006

[21] Kappari, L., Applegate, T.J., Glenn, A.E., Bakre, A. and Shanmugasundaram, R.

(2024) Early Biomarkers for Detecting Subclinical Exposure to Fumonisin B1, Deoxynivalenol, and Zearalenone in Broiler Chickens. *Toxins*, **17**, Article 1. https://doi.org/10.3390/toxins17010001

[22] Abrar, S., Hafeez, A., Rahim, S., Doi, S.A.R. and Khan, M.N. (2025) Effectiveness of a Distance-Learning vs Standard Training in the Integrated Management of Childhood Illnesses: A Cluster Randomized Controlled Trial. *BMC Public Health*, **25**, Article No. 2521. https://doi.org/10.1186/s12889-025-21771-y

[23] De Angelis, N., Amaroli, A., Lagazzo, A., Barberis, F., Zarro, P.R., Cappelli, A., *et al.* (2023) Multipotent Mesenchymal Cells Homing and Differentiation on Poly(ε-Caprolactone) Blended with 20% Tricalcium Phosphate and Polylactic Acid Incorporating 10% Hydroxyapatite 3d-Printed Scaffolds via a Commercial Fused Deposition Modeling 3D Device. *Biology*, **12**, Article 1474. https://doi.org/10.3390/biology12121474

[24] Wüster, J., Neckel, N., Sterzik, F., Xiang-Tischhauser, L., Barnewitz, D., Genzel, A., *et al.* (2024) Effect of a Synthetic Hydroxyapatite-Based Bone Grafting Material Compared to Established Bone Substitute Materials on Regeneration of Critical-Size Bone Defects in the Ovine Scapula. *Regenerative Biomaterials*, **11**, rbae041. https://doi.org/10.1093/rb/rbae041

[25] Wang, Y., Luo, S., Zhang, D., Qu, X. and Tan, Y. (2017) Sika Pilose Antler Type I Collagen Promotes BMSC Differentiation via the ERK1/2 and p38-MAPK Signal Pathways. *Pharmaceutical Biology*, **55**, 2196-2204. https://doi.org/10.1080/13880209.2017.1397177

[26] Rattanpornsompong, K., Rattanaprukskul, K., Prachanukoon, S., Sriwangyang, K., Rinkrathok, M., Tagami, J., *et al.* (2025) Influence of Alloplastic Materials, Biologics, and Their Combinations, along with Defect Characteristics, on Short-Term Intrabony Defect Surgical Treatment Outcomes: A Systematic Review and Network Meta-Analysis. *BMC Oral Health*, **25**, Article No. 413. https://doi.org/10.1186/s12903-025-05782-0